Weightless experiments to probe universality of fluid critical behavior

C. Lecoutre, R. Guillaument, S. Marre, Y. Garrabos, D. Beysens, and I. Hahn

Phys. Rev. E **91**, 060101 — Published 8 June 2015

DOI: 10.1103/PhysRevE.91.060101

Weightless experiments to probe universality of the fluid critical behavior

C. Lecoutre[1,2], R. Guillaument[1,2], S. Marre[1,2], Y. Garrabos[1,2], D. Beysens[3], I. Hahn[4]
[1] *CNRS, ICMCB ESEME, UPR 9048, F-33600 Pessac, France*
[2] *Univ. Bordeaux, ICMCB, UPR 9048, F-33600 Pessac, France*
[3] *ESEME-CEA, Laboratoire de Physique et Mécanique des Milieux Hétérogènes, UMR CNRS-ESPCI ParisTech, Université Paris 6-7, 10 rue Vauquelin, F-75231 Paris Cedex 5, France and*
[4] *Jet Propulsion Laboratory, California Institute of Technology, CA 91109, USA*

Near the critical point of fluids, critical opalescence results in light attenuation, or turbidity increase, that can be used to probe universality of critical behavior. Turbidity measurements in SF_6 under weightlessness conditions on board the International Space Station are performed to appraise such behavior in terms of both temperature and density distances from the critical point. Data is obtained in a temperature range, far (1K) from and extremely close (few µK) to the phase transition, unattainable from previous experiments on Earth. Data is analyzed with renormalization group matching, classical-to-critical crossover models of the universal equation-of-state. It results that the data in the unexplored region, which is a minute deviant from the critical value, still shows adverse effects for testing true asymptotic nature of the critical point phenomena.

PACS numbers: 81.70.Ha, 05.70.Jk, 64.60.fd, 78.35.+c

Thermodynamic and transport properties show singularities asymptotically close to the critical points of many different systems. The current theoretical paradigm on critical phenomena using renormalization group (RG) approach [1] has ordered these systems in well-defined universality classes [2] and has characterized the asymptotic singularities in terms of power laws of only two relevant scaling fields [3]. The modern theory of critical phenomena has been reasonably well validated in earlier experimental studies, in particular along the so-called critical paths where one expects that only a single field variable determines the distance to the critical point (see for example the studies of the specific heat singular behaviors in Refs. [4] and [5] for the $O(1)$ and $O(2)$ universality classes [6], respectively). Simultaneously, the quest of such a *true asymptotic* behavior has been a conundrum to the experimentalists performing experiments closer and closer to the critical point, especially for the case of the gas-liquid critical point of simple fluid-systems. For example, gravity effects on Earth's and long density equilibration times are some of the encountered experimental difficulties in studying the fluid's asymptotic critical behavior [7], which belongs to the universality class of the $N = 1$-vector model of three-dimensional (3D) Ising-like systems and the $O(1)$ symmetric $\left(\Phi^2\right)^2$ field theory [2, 6, 8]. In fact, Earth's-based experiments are typically restricted to a temperature range $\Delta\tau^* = \frac{T}{T_c} - 1 \geq 10^{-4}$, with ($T_c$) T being the (critical) temperature. In this situation, the analytical backgrounds and the classical-to-critical crossover behavior due to the mean-field-like critical point, further hindered the test of the asymptotic Ising-like fluid behavior. Such difficulties are intrinsically unavoidable, even along the true critical paths where the crossover contribution due to one additional non-relevant field [9] can be accounted for correctly in the field theory framework [10, 11]. This intrinsic difficulty associated with the above limited finite temperature range has been shown in the recent re-analysis of critical xenon data [12] from the Earth's experiment performed by Güttinger and Cannell [13].

Practically, the experiments performed even in microgravity environments to avoid gravity effects, are never exactly on these critical paths. Even though the temperature can be made much closer to T_c, the mean density of the fluid cell is never at its exact critical density value. The error-bar related to this latter critical parameter was never contributing to the discussion of the results in terms of true experimental distance to the critical point. As a result, the experimental control of the exact value of the second relevant field was never carefully accounted for in the expected asymptotic Ising-like behavior of the fluid in the close vicinity of its gas-liquid critical point. For instance, in our previous light transmission and turbidity (τ) measurements [14] performed in near-critical SF_6 under microgravity environments, it was noted that the finite small value ($\sim 0.8\%$) of the off-density criticality could be one of the reasons to explain the increasing small differences between the experimental data and the theoretical estimates referring to the so-called Ornstein-Zernike (OZ) theory [15] along the critical isochoric path.

Here we would like to probe critical point universality along a non-critical path by using over three hundred data points obtained in twelve runs of near-critical SF_6 turbidity measurements in weightless condition. More precisely, the 327 new turbidity data were obtained from March 2011 to February 2014 using the SF_6 sample at constant ($\sim$ 1%) off-critical density (see below) of the ALI insert in the CNES-NASA DECLIC facility onboard the International Space Station (ISS). This cell was purposefully filled at off-critical, liquid-like density for studying boiling phenomena in the two-phase range (see [16] for details), taking thus benefit of the liquid wettability on the cell walls and sapphire windows. Nonetheless, the light transmission and turbidity (τ) measurements on the

one-phase domain have provided a new unique set of data valuable to check our novel approach of the theoretical estimates referring to the fluid singular behavior along a non-critical path. The DECLIC instrument [17] is an advanced optical, thermal, and mechanical facility which uses different inserts dedicated to the studies, without the gravity effects, of the critical point phenomena and the boiling, the solvatation-precipitation, or the solidification mechanisms in transparent media.

The ALI-DECLIC turbidity measurements were performed very close to the critical point, nearly three orders of magnitude in temperature distance beyond what has been achieved previously on Earth's, by taking advantages of the high level performances of the facility. These turbidity measurements along a non-critical path, comparable to the ones reported in Ref. [14], can now be analyzed with a much improved theoretical understanding than in earlier OZ framework studies. The two data sets are in fact different and independently essential in testing our novel crossover models of the equation-of-state [12] based on the RG approaches of the critical phenomena universality. Indeed, the crossover parametric model (CPM) [18] of the equation of state, although phenomenological, presents the main advantage in calculating the singular thermodynamic properties in any point of the density-temperature phase surface in the close vicinity of the gas-liquid critical point. Despite small numerical differences between universal quantities, the massive renormalization crossover functions and CPM, both showed similar Ising-like critical behaviors, only characterized by three fluid-dependent parameters (de facto Ising-like in nature). Moreover, it was also shown in critical xenon case [12] that CPM can be modified into the crossover master model (CMM) with no adjustable Ising-like critical parameter, since the phenomenological master forms of the crossover functions and CMM only involves the known critical point coordinates [11]. CMM can then also be used to predict the asymptotic singular behaviors in the near-critical phase region surrounding a well-localized gas-liquid critical point of any one-component fluid.

Turbidity measurements. We briefly recall that the ALI-DECLIC turbidity experiments used the attenuation of the intensity of the DECLIC laser light (wavelength $\lambda_0 = 632.8\,\mathrm{nm}$, focal beam size 0.3 mm, maximum attenuation of the 1 mW power), crossing the central axis of the direct observation cell (DOC) of the ALI insert. Therefore, $\tau_{\rm exp} = -\frac{\ln(R_I)}{e} + B_\tau$ expresses the light intensity attenuation per unit length through the measurements of the intensity ratio $R_I = I_2/I_1$, where I_1 is the incident laser light intensity from the entrance optics, I_2 is the related transmitted one through the fluid layer, and e is the fluid layer thickness. B_τ is an adjustable constant that accounts for components in the optical path ($B_\tau \simeq 100 \pm 0.5\,\mathrm{m}^{-1}$ for the DECLIC optical design). The DOC (ten years old at near-critical density filling) was described in [16]. Three main DOC characteristics are of present interest. (i) DOC has a fixed cylindrical-like fluid volume of $D = 10.6\,\mathrm{mm}$ in diameter and $e = 4.115\,\mathrm{mm}$ in thickness. (ii) The fluid under study was SF_6 of electronic quality, corresponding to a 99.98% purity (from Alpha Gaz - Air Liquide); (ii) DOC was initially filled at a mean liquid-like density $\langle\rho\rangle$, i.e., $\langle\rho\rangle > \rho_c$, with well-controlled relative off-critical density $\langle\delta\tilde{\rho}\rangle = \frac{\langle\rho\rangle}{\rho_c} - 1 = (1 \pm 0.2)$ % from Earth based filling and checking processes. This last point will be detailed in a separate analysis including recent post-flight data.

The laser light transmission measurements were also used to determine the relative coexistence temperature $T_{\rm coex} < T_c$. The temperature difference $T_c - T_{\rm coex} \simeq 55\,\mu\mathrm{K}$ was estimated using the power law $\Delta\tilde{\rho}_{LV} = B\,(\Delta\tau^*)^\beta$ describing the symmetrized top of the coexistence curve, with $\Delta\tilde{\rho}_{LV} = \langle\delta\tilde{\rho}\rangle$ and $\Delta\tilde{\rho}_{LV} = \frac{\rho_L - \rho_V}{2\rho_c}$, $B = 1.596$, $\beta = 0.32575$ and $T_c\,(\mathrm{SF_6}) = 318733.000\,\mathrm{mK}$ [14]. ρ_L and ρ_V are the coexisting liquid and vapor densities, respectively. Note that the absolute calibration of the temperature sensors of the thermostat was not required determining $T_{\rm coex}\,(\mathrm{SF_6})_{\rm ALI}$, which can then be used as a relative reference for the temperature scale associated to the ALI-DECLIC set up. In this case, the thermal monitoring by the DECLIC facility gives a relative temperature uncertainty of the order of 15 μK, with a temperature resolution of 1 μK during the complete duration of the experimental run. Therefore, our turbidity data were obtained from a few μK to 1 K above $T_{\rm coex}$ (i.e., $10^{-7} \leq \Delta\tau^*_{\rm coex} = \frac{T}{T_{\rm coex}} - 1 \leq 3.1 \times 10^{-3}$). Note that the methodology for performing these ALI-DECLIC turbidity experiments remains similar to the one for ALICE2 experiments in the MIR station (see Ref. [14]). The major improvement results from the use of an upgraded temperature timeline in DECLIC, which has taken great benefit of the CADMOS and NASA teleoperational managing of this facility. That was especially noticeable on the (at least) two-days duration of the final part of the timeline where the last decade $T - T_{\rm coex} \leq 1.2\,\mathrm{mK}$ was covered by performing a serie of $-100\,\mu\mathrm{K}$ temperature depth quenches, of at least 4 hours relaxation period each. Therefore by combining the μK resolution with the 15 μK uncertainty, a typical error bar of 30 μK can be attributed to the data point in the closest temperature range. An upcoming detailed paper will describe this preparation of a homogeneous thermodynamic state of a near-critical fluid sample in weightlessness conditions at the closest temperature above the two phase domain (i.e., a few μK to $\sim 50\,\mu$K above $T_{\rm coex}$, typically).

Our 327 $\tau_{\rm exp}$ data are reported as functions of $T - T_{\rm coex}$ in Fig. 1, noting that 85 data are in the range $T - T_{\rm coex} \leq 1\,\mathrm{mK}$ and that the temperature range not affected by gravity on a similar Earth experiment is restricted to $T - T_{\rm coex} \geq 38\,\mathrm{mK}$ [19]. The symbols defined in the inserted table of Fig. 1 correspond to the twelve series of ALI-DECLIC turbidity data. Each serie corresponds to a typical, about five-day duration, temperature timeline, performed during the different sequences, which covers the temperature range $T_{\rm coex} + 1\,\mathrm{K} \rightarrow T_{\rm coex}$. In Fig. 1, we

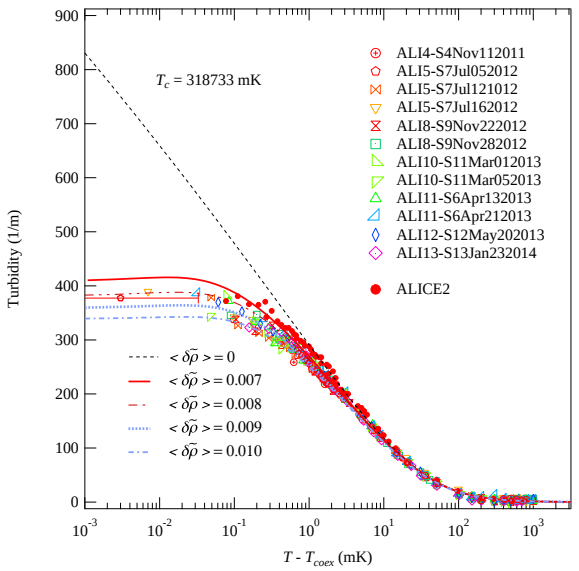

Figure 1: (color online) lin-log plot of turbidity τ (expressed in m^{-1}) as a function of $T - T_{\rm coex}$ (expressed in mK) obtained from present ALI-DECLIC and previous ALICE2 light transmission measurements in SF_6 (symbols are given in the inserted table) and compared to the predicted turbidity from Eq. (2), using the CMM equation-of-state model with calculated parameters from column 3 of Table I. Black dashed curve represents Eq. (2) for $\langle\delta\tilde{\rho}\rangle = 0$ (exact critical isochore). The additional four (red full, red dot-dot-dashed, blue dotted, blue dot-dashed) curves represent Eq. (2) for $\langle\delta\tilde{\rho}\rangle$ covering the 0.7 to 1.0%-range, by using 0.1% steps, respectively. The typical 30 μK temperature error-bar is only indicated by a horizontal red bar for the closest data point ($T - T_{\rm coex} \sim 3\,\mu$K).

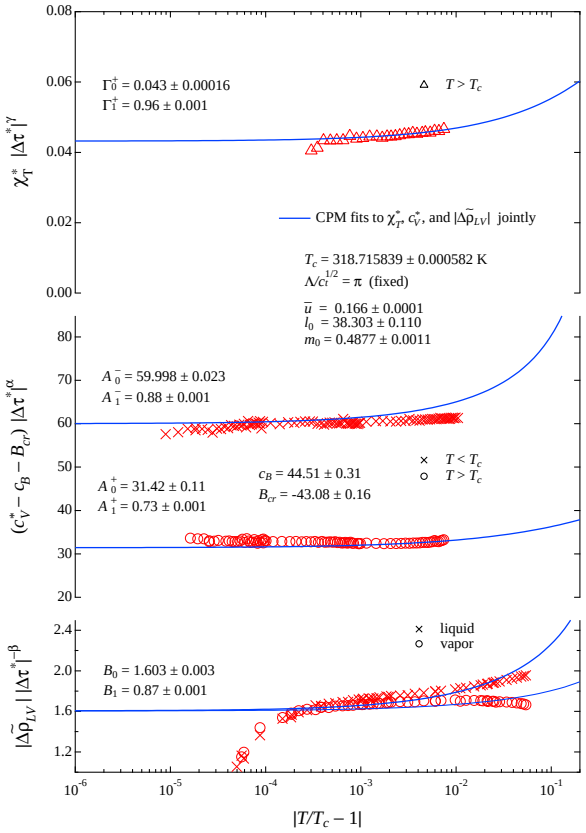

Figure 2: (color online) A joint fit result for the free parameters l_0, m_0 and $\overline{u}$ of the CPM model fitting the SF_6 $\chi_T^* = \kappa_T p_c$, c_V^*, and $\Delta\tilde{\rho}_{LV}$ measurements of Refs. [22], [4], and [23], respectively, as functions of $|\Delta\tau^*|$ along the critical isochore (see Ref. [18] for the amplitude notations and inserted labels for the curves and the symbols).

have also added our previous turbidity data (as the form of red full circles) obtained from the ALICE2 turbidity experiments [14], using a cell with off-density criticality $\langle\delta\tilde{\rho}\rangle_{\rm ALICE2} = (0.8 \pm 0.1)$ %.

Turbidity functional forms for a near-critical fluid. Turbidity of a fluid close to its liquid-gas critical point is most essentially due to Rayleigh light scattering by density fluctuations. τ measurements as a function of the distance from the critical point allow Ising-like asymptotic formulations for the static isothermal compressibility (κ_T, governed by the critical exponent γ along the critical isochore) and the correlation length (ξ, governed by the critical exponent ν along the critical isochore) to be checked. Indeed, from the detailed analysis given in [12], τ can be written in the following scaling form

$$\tau = \frac{\pi A_0 k_B T \kappa_T}{y^2} H(\eta, y) \qquad (1)$$

where $A_0 = \frac{\pi^2}{\lambda_0^4}\left[\frac{(n^2-1)(n^2+2)}{3}\right]^2$ and n is the fluid refractive index. k_B is the Boltzmann constant. $y = k_0\xi$ is universal (non-dependent of the normalization) and $k_0 = \frac{2\pi n}{\lambda_0}$ is the amplitude of the incident light wave vector ($\sim 10^{-7}\,m^{-1}$ for $\lambda_0 \sim 632.8$ nm). $H(\eta, y)$ is the turbidity scaling function, which is universal as y is, the critical exponent η satisfying thus the hyper-scaling law $\gamma = 2\nu - \eta\nu$. As shown in [12], when $T \to T_c$, i.e. $y \gg 1$ or $x \to \infty$, only the asymptotical critical behavior of $H(\eta, y)$ must be explicited as a function of the critical exponent η. In term of usual Ising-like power law along the critical isochore, i.e., for $y \gg 1$ and $\Delta\tau^* \to 0$, $H(\eta, y) \propto F \times (\Delta\tau^*)^{-\eta\nu}$ where F is an universal quantity. F is thus related to the saturated finite turbidity at the exact critical point, such as $\tau \sim \frac{cte}{\eta}$, as shown by the asymptotic analysis of Ferrell [20]. However, the Ferrell's asymptotic analysis, as well as its confirmation by the Martin-Mayor et al Monte Carlo simulation of a simple cubic Ising lattice [21], leads to Ising-like limiting forms of the turbidity expected only valid for $\Delta\tau^* < 10^{-5}$, i.e. very close to the critical temperature. At large distance from T_c, when $x \leq 1$, the turbidity reduces to the Puglielli and Ford [19] estimation from the OZ theory. In such a second limiting case, Eq. (1) takes the practical functional form $\tau_{\rm PF} = \frac{\pi A_0 k_B T \kappa_T}{y^2} H_{\rm PF}(y)$, with $H_{\rm PF}(y) =$

$\frac{1}{8y^4}\left[\left(8y^4+4y^2+1\right)\ln\left(1+4y^2\right)-4y^2\left(1+2y^2\right)\right]$. The ratio $\frac{H_{\rm PF}(y)}{y^2}$ reaches the constant value $\frac{8}{3}$ for $y \ll 1$, leading to $\tau_{\rm PF}=\tau_0\left(1+\Delta\tau^*\right)\left(\Delta\tau^*\right)^{-\gamma} \propto T\kappa_T$ far away from T_c. $\tau_0=\pi A_0 k_B T_c \Gamma_0^+$ is a temperature independent quantity, only proportional to the leading amplitude Γ_0^+. Unfortunately, for a 3D Ising system, $H\left(\eta,y\right)$ always remains unknown between the above two limiting behaviors. Therefore, in our modelling we consider the phenomenological fitting formulation proposed by Martin-Mayor et al [21] to reproduce the crossover between the turbidity results of the Monte Carlo simulation (close to T_c) and the ones of the PF approximation (far from T_c), such as

$$\tau_{\rm MM,fit} = \tau_{\rm PF}\left[0.666421+0.242339\left(1+0.0087936y^2\right)^{\frac{\eta}{2}} +0.0911801\left(1+0.09y^4\right)^{\frac{\eta}{4}}\right] \quad (2)$$

This fitting form recovers the condition $\tau_{\rm MM,fit}\sim\tau_{\rm PF}$ far from the critical temperature ($y\leq 1$ or $\Delta\tau^*\geq 10^{-5}$).

Estimations of ξ, κ_T, and τ for near-critical SF_6. Our calculations of $\kappa_T\left(\Delta\tau^*,\langle\delta\tilde{\rho}\rangle\right)$, $\xi\left(\Delta\tau^*,\langle\delta\tilde{\rho}\rangle\right)$ and $\tau\left(\Delta\tau^*,\langle\delta\tilde{\rho}\rangle\right)$ for the near-critical ($\langle\delta\tilde{\rho}\rangle\neq 0$) SF_6 case are similar to the critical ($\langle\delta\tilde{\rho}\rangle=0$) Xe case reported in [12]. First, the CPM free adjustable parameters (l_0, m_0 and $\overline{u}$) for SF_6 are obtained from a joint fitting of isothermal compressibility [22], heat capacity at constant volume [4], and coexisting density curve [23]. The results are shown in Fig. 2, where only the reduced temperature range of the c_V data obtained in microgravity reaches the $10^{-5}-10^{-4}$ decade. Second, the corresponding CMM fixed parameters are obtained from the following relations

$$\begin{aligned} l_0 &= \frac{3.38317}{\mathcal{Z}_\chi^+}\frac{\mathcal{Z}_M}{3.28613}\left(Z_c\right)^{\frac{1}{2}}\left(Y_c\right)^{\beta+\gamma} \\ m_0 &= \frac{\mathcal{Z}_M}{3.28613}\left(Z_c\right)^{-\frac{1}{2}}\left(Y_c\right)^{\beta} \\ \left[\overline{u}\pi\right]^{-2\Delta_s}\left(1-\overline{u}\right) &= \frac{\mathcal{Z}_\varkappa^{1+}}{0.590}\left(Y_c\right)^{\Delta} \end{aligned} \quad (3)$$

neglecting quantum effects for the SF_6 case and using the arbitrary relation $\frac{\Lambda}{\left(c_t\right)^{\frac{1}{2}}}=\pi$ initially adopted by the authors in Ref. [18]. $\mathcal{Z}_\chi^+=0.11975$, $\mathcal{Z}_M=0.4665$, and $\mathcal{Z}_\varkappa^{1+}=0.555$ [11]. Table I shows that the free (column 2) and fixed (column 3) values are in close-agreement.

Our theoretical estimation of τ using Eq. (2) with CMM parameters (column 3, Table I) to calculate ξ and κ_T for $\langle\delta\tilde{\rho}\rangle=0$, corresponds to the black dashed curve in a log-lin scale of Fig. 1. The additional four curves correspond to the similar predictive modelling for four near-critical isochores covering the $\langle\delta\tilde{\rho}\rangle=(0.7\,\text{to}\,1.0)\,\%$-range, using four 0.1% steps (see the inserted curve labels in Fig. 1). This $\langle\delta\tilde{\rho}\rangle$-range includes the experimental central values $\langle\delta\tilde{\rho}\rangle_{\rm ALI}=1\,\%$ and $\langle\delta\tilde{\rho}\rangle_{\rm ALICE2}=0.8\,\%$.

Discussion. Figure 1 indicates that the τ calculations from Eq. (2), without adjustable parameter, are in agreement with our experimental data using $\langle\delta\tilde{\rho}\rangle\approx 0.9\%$ (blue dotted curve) for the present ALI-DECLIC case and $\langle\delta\tilde{\rho}\rangle\approx 0.7\%$ (red full curve) for the previous ALICE2 case. This good agreement is noticeable in the temperature range $T-T_{\rm coex}\lesssim 25\,\text{mK}$ never investigated experimentally until now as a function of $\langle\delta\tilde{\rho}\rangle$, whereas the estimated small differences ($\sim -0.1\%$) from the above central values are in the same order of magnitude as the experimental error-bar. In addition, complementary fits of the τ data (ALI-DECLIC+ALICE2), fixing $\overline{u}=0.166$ (joint fit value) with l_0, m_0 and $\langle\delta\tilde{\rho}\rangle$ as the free parameters, lead to the results reported in column 4 of Table I. The l_0 and m_0 differences from column 2 could be easily understood by considering the limited available data range of the joint fit, compared to the one of the turbidity data. Similarly, the $\langle\delta\tilde{\rho}\rangle$ values agree with an uncertainty $\sim 0.1\%$.

SF_6	CPM Joint fit	CMM	Turbidity fit (this work)
l_0	38.303 ± 0.110	36.1923	36.472±0.694
m_0	0.4877 ± 0.001	0.48568	0.4915±0.001
$\bar{u}$	0.166 ± 0.0001	0.124284	0.166 (fixed)
$\Lambda\left(c_t\right)^{\frac{1}{2}}$	π (fixed)	π (fixed)	$\langle\delta\tilde{\rho}\rangle_{\rm ALI}=(0.95\pm0.05)\,\%$
$g^{\frac{1}{2}}$	0.5215 ± 0.0001	0.39045	$\langle\delta\tilde{\rho}\rangle_{\rm ALICE2}=(0.75\pm0.17)\,\%$

Table I: Sulfurhexafluoride values of the Ising-like parameters l_0, m_0 and $\overline{u}$ for CPM joint fit (see Fig. 2), CMM (see Eqs. (3) and text), and fitting the turbidity data with $\bar{u}=0.166$, $\Lambda\left(c_t\right)^{\frac{1}{2}}=\pi$ (fixed) and l_0, m_0, and $\langle\delta\tilde{\rho}\rangle$ as free parameters (see text).

The current analysis shows that the off-critical density of the cell is the dominant effect which explains the observed increasing deviation from the critical singular behavior of the turbidity approaching T_c, thanks to the microgravity environment and the high-level capabilities of ALI-DECLIC for experimenting accurately at temperature distances lower than 1 mK from $T_{\rm coex}$. Here, the multiple scattering effect is considered to be a negligible factor ($<10\%$) in our forward scattering case ($\theta<2.7°$) [24]. Moreover, the intrinsic gravitational effects in the sample fluid at the size of the laser beam, which could limit the growth of the correlation length on Earth, are insignificant in microgravity conditions even at the reduced temperature of 10^{-7}[7].

The modelling of τ is comparable (in amplitude and uncertainty) to the three sets of Ising-like parameters given in Table I. In addition, the estimated off-criticality values of the cell densities are in agreement with Earth-based experimental determinations. Finally, in a temperature-density range very close to ρ_c and T_c which has never been investigated until now, the turbidity behavior is reasonably well understood from the use of the parametric form of the equation of state without any adjustable parameter. This modelling approach is made in conformity with the Ising-like universality features of the massive renormalization scheme, only knowing the SF_6 generalized critical coordinates.

Acknowledgments We thank all the DECLIC, CNES, NASA, and associated industrial teams involved in the ALI-DECLIC project development and achievement, and in particular the NASA and CADMOS teams for operational managing and control of the facility onboard the ISS. CL, RG, SM, YG, and DB, are grateful to CNES for financial support. The research (IH) was carried out at Jet Propulsion Laboratory, California Institute of Technology, under a contract with NASA.

[1] K. G. Wilson, Rev. Mod. Phys., **47,** 776 (1975).
[2] J. Zinn-Justin, *Quantum Field Theory and Critical Phenomena*, 4^{th} ed. (Clarendon, Oxford, 2002).
[3] M. E. Fisher, J. Math. Phys. **5**, 944 (1964).
[4] A. Haupt and J. Straub, Phys. Rev. E **59**, 1795 (1999).
[5] J. A. Lipa, D. R. Swanson, J. A. Nissen, Z. K. Geng, P. R. Williamson, D. A. Stricker, T. C. P. Chui, U. E. Israelsson, and M. Larson, Phys. Rev. Lett. **84**, 4894 (2000).
[6] M. Barmatz, I. Hahn, J.A. Lipa, R.V. Duncan, Rev. Mod. Phys., **79**,1 (2007).
[7] M. R. Moldover, J. V. Sengers, R. W. Gammon and R. J. Hocken, Rev. Mod. Phys., **51**, 79 (1979).
[8] M. A. Anisimov and J. V. Sengers, in *Equations of State for Fluids and Fluid Mixtures*, part I, edited by J. V. Sengers, R. F. Kayser, C. J. Peters, and H. J. White, Jr. (Elsevier, Amsterdam, UK, 2000), pp. 381-434, and references therein.
[9] F. J. Wegner, Phys. Rev. B **5**, 4529 (1972).
[10] C. Bagnuls and C. Bervillier, Phys. Rev. E **65**, 066132 (2002).
[11] Y. Garrabos and C. Bervillier, Phys. Rev. E **77**, 021116 (2008).
[12] Y. Garrabos, C. Lecoutre, S. Marre, D. Beysens, and I. Hahn, J. Stat. Phys. **158**, 1379-1412 (2015).
[13] H. Güttinger and D. S. Cannell, Phys. Rev. A **24**, 3188 (1981).
[14] C. Lecoutre, Y.Garrabos, E. Georgin, F. Palencia, D. Beysens, Int. J. Thermophys. **30**, 810-832 (2009).
[15] L. S. Ornstein and F. Zernike, Proc. Acad. Sci. Amsterdam, **17**, 793 (1914); Phys. Z, **19**, 134 (1918).
[16] Y. Garrabos, C. Lecoutre, D. Beysens, V. Nikolayev, S. Barde, G. Pont, B. Zappoli, Acta Astronautica **66**, 760–768 (2010).
[17] see http://smsc.cnes.fr/DECLIC/index.htm
[18] V. A. Agayan, M. A. Anisimov, and J. V. Sengers, Phys. Rev. E **64**, 026125 (2001).
[19] V. G. Puglielli and N. C. Ford, Phys. Rev. Lett. **25**, 143 (1970).
[20] R. A. Ferrel, Phys. A **177**, 201-206 (1991).
[21] V. Martin-Mayor, A. Pelissetto, and E. Vicari, Phys. Rev. E **66**, 026112 (2002).
[22] G. T. Feke, G. A. Hawkins, J. B. Lastovka, and G. B. Benedek, Phys. Rev. Lett. **27**, 1780 (1971).
[23] J. Weiner, Ph.D. thesis, 1974.
[24] A. Bailey and D. S. Cannell, Phys. Rev. E **50**, 4853 (1994).